Existence of bulk chiral fermions and crystal symmetry

J. L. Mañes

Departamento de Física de la Materia Condensada, Universidad del País Vasco, Apartado 644, E-48080 Bilbao, Spain

We consider the existence of bulk chiral fermions around points of symmetry in the Brillouin zone of nonmagnetic three-dimensional (3D) crystals with negligible spin-orbit interactions. We use group theory to show that this is possible, but only for a reduced number of space groups and points of symmetry that we tabulate. Moreover, we show that for a handful of space groups the existence of bulk chiral fermions is not only possible but unavoidable, irrespective of the concrete crystal structure. Thus our tables can be used to look for bulk chiral fermions in a specific class of systems, namely, that of nonmagnetic 3D crystals with sufficiently weak spin-orbit coupling. We also discuss the effects of spin-orbit interactions and possible extensions of our approach to Weyl semimetals, crystals with magnetic order, and systems with Dirac points with pseudospin 1 and 3/2. A simple tight-binding model is used to illustrate some of the issues.

I. INTRODUCTION

Electrons in the vicinity of the K points in graphene[1,2] have linear dispersion relations and behave like massless chiral fermions. More concretely, the dynamics of electrons around these points is governed by the relativistic, two-dimensional, massless Dirac Hamiltonian $H_0 \sim \sigma_x k_x + \sigma_y k_y$, and many of the exotic electronic properties of graphene stem from this fact.[3] This also turns graphene into a potential laboratory for two-dimensional relativistic dynamics, incorporating massless fermions, gauge fields, and curved gravitational backgrounds.[4] Moreover, optical lattices that could be used to simulate relativistic systems with trapped cold atoms can be fashioned after graphene,[5] with control over the properties of the system.[6,7] Obviously three-dimensional analogs of graphene are potentially very interesting.

Strictly speaking, the massless Dirac Hamiltonian H_0 describes only the low-energy *orbital* dynamics of electrons in graphene. As reviewed in Sec. III, spin-orbit coupling in graphene gives fermions a very small mass.[8] This mass is so small that for most practical purposes the spin and orbital degrees of freedom decouple and H_0 provides an effective description of an enormous variety of phenomena.[3]

In this paper we will consider three-dimensional (3D) analogs of graphene, i.e., crystals with orbital electron dynamics governed by the 3D two-component massles Dirac Hamiltonian $H_0 \sim v\vec{\sigma} \cdot \vec{k}$, also known as the Weyl Hamiltonian. This Hamiltonian describes massless chiral fermions, right handed for $v > 0$ and left handed otherwise. Henceforth we will use the term "orbital Weyl point" to refer to points around which the low-energy dynamics in the absence of spin-orbit couplings is described by the 3D Weyl Hamiltonian, with an additional twofold degeneray due to electron spin. We will also speak of "bulk chiral fermions," keeping in mind that, as in graphene,[3] they are exactly chiral in the limit of vanishing spin-orbit interactions. Also note that it is *pseudospin*, not electron spin, which is parallel (or antiparallel) to $\vec{k}$ in the chiral limit and that, in these systems, pseudospin is purely orbital in origin.

These should be distinguished from other systems where the *total* Hamiltonian, including electron spin and spin-orbit interactions, adopts the form of the Weyl Hamiltonian. These include surface states in topological insulators[9] as well as novel three-dimensional "Weyl semimetals."[10–15] The spectrum of these systems, unlike those of graphene and its 3D analogs considered in this paper, remains gapless for arbitrary values of the spin-orbit couplings. Actually, some Weyl semimetals have *strong* spin-orbit interactions.[12] Possible extensions of our methods to Weyl semimetals will be considered in the last section.

It is well known that Weyl points have topological properties,[16–18] and no fine tuning or symmetries are usually necessary for their existence. But symmetry, even if not necessary,[19] can sometimes be *sufficient* for the existence of Weyl points. That is what we show in this paper, where we investigate the role played by the space groups of crystals with time-reversal symmetry (TRS) in the existence of orbital Weyl points.

The main results of this paper are summarized in Tables I and II. Only crystals with one of the 19 space groups in these tables *can* have orbital Weyl points at points of symmetry. Moreover, crystals with space groups in Table I *must* have orbital Weyl points at the listed points, *irrespective of the actual crystal structure*. For crystals with space groups in Table II the situation is only slightly different: At the listed points both orbital Weyl points and nondegenerate bands with quadratic dispersion relations are possible. These results are relevant to nonmagnetic 3D crystals with sufficiently weak spin-orbit interactions and to cold atoms in optical lattices.

The rest of the paper is organized as follows. Our main results, contained in Eq. (2) and Tables I and II are explained in Sec. II. Section III considers the effects of spin-orbit interactions on the orbital Weyl points, and a simple tight-binding model is constructed and analyzed in Sec. IV. Possible extensions of our approach to Weyl semimetals, crystals with magnetic order, and other types of Dirac points are considered in Sec. V. An outline of the methods used to obtain Tables I and II is given in the Appendix.

II. ORBITAL WEYL POINTS AND CRYSTAL SYMMETRY

Our strategy is based on the fact that the form of the Hamiltonian in the vicinity of a point of symmetry $\vec{K}_1$ is strongly constrained by the symmetries of the point in

TABLE I. Cubic, tetragonal, and orthorhombic space groups with orbital Weyl points. The small IRs are all 2d (except for R_3 of **212** and **213**, which is 4d) and refer to the symmetry points $P(\frac{1}{4},\frac{1}{4},\frac{1}{4})$, $R(\frac{1}{2},\frac{1}{2},\frac{1}{2})$, $A(\frac{1}{2},\frac{1}{2},\frac{1}{2})$, and $W(\frac{3}{4},\frac{1}{4},\frac{1}{4})$, with components in the conventional basis of Ref. 26. The stars have two vectors $(\vec{K}_1, -\vec{K}_1)$ for body-centered (I) lattices and a single vector $\vec{K}_1 \equiv -\vec{K}_1$ for simple (P) lattices.

Space group			IRs
214	$I4_132$	O^8	P_1, P_2, P_3
213	$P4_132$	O^7	R_1, R_2, R_3
212	$P4_332$	O^6	R_1, R_2, R_3
199	$I2_13$	T^5	P_1, P_2, P_3
198	$P2_13$	T^4	R_1, R_2, R_3
098	$I4_122$	D_4^{10}	P_1
096	$P4_32_12$	D_4^8	A_1, A_2
092	$P4_12_12$	D_4^4	A_1, A_2
024	$I2_12_12_1$	D_2^9	W_1
019	$P2_12_12_1$	D_2^4	R_1

question.[20–23] These include $\mathcal{G}_{K_1}$—the little group[24,25] of the vector $\vec{K}_1$—and combinations of TRS with space group elements. Since we are interested in systems with very weak spin-orbit interactions, we will consider first the structure of the orbital or spin-independent part of the Hamiltonian. The transformation properties of orbital wave functions are described by single-valued[26] representations of the space group.

As explained in the Appendix, we have carried out a survey of all the single-valued irreducible representations of the 230 space groups at points of symmetry in the Brillouin zone (BZ). We find that, for most space groups, the constraints on the form of the Hamiltonian around points of symmetry are incompatible with the structure of the Weyl Hamiltonian. The comparatively few exceptions are listed in Tables I and II. In all cases, two electronic bands transforming according to a single-valued irreducible representation (IR) of $\mathcal{G}_{K_1}$ are degenerate at the point of symmetry $\vec{K}_1$. Near the point of symmetry, i.e., for $\vec{K} = \vec{K}_1 + \vec{k}$, the degeneracy is broken by

TABLE II. Hexagonal and trigonal space groups with orbital Weyl points. The small IRs listed are all 2d and refer to the symmetry points $K(\frac{\bar{1}}{3},\frac{2}{3},0)$ and $H(\frac{\bar{1}}{3},\frac{2}{3},\frac{1}{2})$, with components in the conventional basis of Ref. 26 The stars have two vectors $(\vec{K}_1, -\vec{K}_1)$ in all cases.

Space group			IRs
182	$P6_322$	D_6^6	K_3
181	$P6_422$	D_6^5	K_3, H_3
180	$P6_222$	D_6^4	K_3, H_3
179	$P6_522$	D_6^3	K_3
178	$P6_122$	D_6^2	K_3
177	$P622$	D_6^1	K_3, H_3
154	$P3_221$	D_3^6	K_3, H_3
152	$P3_121$	D_3^4	K_3, H_3
150	$P321$	D_3^2	K_3, H_3

$\vec{k}$-dependent terms and the Hamiltonian takes the form

$$H(\vec{k}) = v_x \sigma_x k_x + v_y \sigma_y k_y + v_z \sigma_z k_z + O(k^2), \qquad (1)$$

where $v_x = v_y$ for uniaxial crystals and $v_x = v_y = v_z$ for cubic crystals. After appropriate rescalings of the components of $\vec{k}$ for nonisotropic crystals, this is just the Weyl Hamiltonian $H \sim v\vec{\sigma} \cdot \vec{k}$, with the sign of v equal to the product of the signs of v_i. The points of symmetry and IRs where this happens are listed in the last column of Tables I and II in standard notation.[26]

TRS reverses the sign of $\vec{K}$. In those cases where $-\vec{K}_1$ is not equivalent to $\vec{K}_1$, we get a copy of the Weyl Hamiltonian at the mirror point $-\vec{K}_1$ and fermions have, in addition to the pseudospin index associated with the Pauli matrices σ_i, a "valley" index. As shown in the Appendix, the total Hamiltonian is then given by the 4×4 matrix

$$H(\vec{k}) = v \begin{pmatrix} \vec{\sigma} \cdot \vec{k} & 0 \\ 0 & \vec{\sigma} \cdot \vec{k} \end{pmatrix} + O(k^2). \qquad (2)$$

This describes two degenerate massless fermions of the *same chirality*, right handed for $v > 0$ and left handed otherwise. Somewhat surprisingly, we find that this doubling continues to take place even when $-\vec{K}_1 \equiv \vec{K}_1$, i.e., for TRS-invariant momenta. In that case, Eq. (2) describes two distinct fermions of the same chirality at the *same point* in the BZ. There is still a valley index but, unlike in graphene, it cannot be associated with two different points in the BZ. This happens for the six space groups with simple (P) Bravais lattices in Table I.

The groups in Table I have one important feature in common: The IRs in the last column of the table include *all* the IRs at the point of symmetry. This means that, at that point, all the bands must form degenerate pairs with Weyl Hamiltonians. In other words, *any* crystal with space group in Table I will have bulk chiral fermions described by Eq. (2), irrespective of the concrete crystal structure. On the other hand, the space groups in Table II have, besides the listed small IRs K_3 and H_3, which are two-dimensional (2d) and give rise to orbital Weyl points, other 1d small IRs (K_1, K_2, H_1, H_2) not related to Weyl points. In this case, both orbital Weyl points and nondegenerate bands with quadratic dispersion relations are possible at the listed points of symmetry.

We close this section by pointing out some special features in Tables I and II. The first one is that all the groups in Table I are subgroups of the first entry,[27,28] the cubic space group **214** $I4_132$ and, despite the use of different conventional names (P, R, A, W), they also share the point of symmetry. Indeed, the Cartesian coordinates for all the points in Table I can be written as

$$\vec{K}_1 = \left(\frac{\pi}{a}, \frac{\pi}{b}, \frac{\pi}{c} \right) \qquad (3)$$

in terms of the unit cell constants, with $b = c$ for uniaxial crystals and $a = b = c$ for cubic crystals. As a result, one can begin with any 3D lattice with space group **214** and reproduce all the cases in Table I by suitable deformations. The second somewhat surprising feature is that all the stars have just one or two vectors. As a consequence, these crystals have only one or two orbital Weyl points degenerate in energy. This should be contrasted, for instance, with the case studied in Ref. 12,

where 24 Weyl points (away from points of symmetry) are present at the Fermi energy.

III. SPIN-ORBIT INTERACTIONS

Strictly speaking, our analysis so far applies only to "spinless electrons." It is well known that spin-orbit interactions in graphene open a gap and give fermionic excitations a small mass.[8] In the case of graphene, the intrinsic spin-orbit Hamiltonian is proportional to $\sigma_z \otimes s_z \otimes \tau_z$, where s_z and τ_z are Pauli matrices for electron spin and valley indices, respectively. Around each valley, the Hamiltonian can be written in terms of 4×4 matrices,

$$H_0 + H_{so} = v(\alpha_x k_x + \alpha_y k_y) + \beta \Delta, \qquad (4)$$

where $\alpha_i = \sigma_i \otimes \mathbf{1}_s$, $\beta = \pm \sigma_z \otimes s_z$, and Δ is the strength of the spin-orbit coupling. The matrices satisfy the Clifford algebra

$$\{\alpha_i, \alpha_j\} = 2\delta_{ij}, \quad \{\alpha_i, \beta\} = 0, \quad \beta^2 = 2. \qquad (5)$$

This identifies Eq. (4) as the Dirac Hamiltonian for four-component fermions with mass $m = \Delta$ and spectrum $E_\pm = \pm\sqrt{\Delta^2 + v^2 k^2}$.

For the space groups in Tables I and II, the most general k-independent spin-orbit Hamiltonian compatible with spatial symmetries and TRS takes the form

$$H_{so} = \tfrac{1}{4}(\Delta_x \sigma_x \otimes s_x + \Delta_y \sigma_y \otimes s_y + \Delta_z \sigma_z \otimes s_z) \otimes \mathbf{1}_\tau, \quad (6)$$

where $\Delta_x = \Delta_y$ for uniaxial crystals and $\Delta_x = \Delta_y = \Delta_z$ for cubic crystals. Actually, this valley-independent form of the spin-orbit interaction is valid on the basis $(e_1, e_2, ie_2^*, -ie_1^*)$ of orbital wave functions introduced in the Appendix. If one uses the more conventional basis (e_1, e_2, e_1^*, e_2^*), then one has to append the valley matrix τ_z to the x and z components in Eq. (6). Note that, in the conventional basis, instead of Eq. (2), we would have Eq. (A6).

The spectrum of the total Hamiltonian $v\vec{\sigma} \cdot \vec{k} + H_{so}$ can be computed numerically, and one finds that, in general, gaps are generated and all fermionic excitations acquire masses. Cubic crystals, where H_{so} is isotropic and depends on a single parameter Δ, are an exception and can be treated analytically. In this case the spectrum is given by

$$E_\pm^- = -\frac{\Delta}{4} \pm \sqrt{\left(\frac{\Delta}{2}\right)^2 + v^2 k^2},$$
$$E_\pm^+ = \frac{\Delta}{4} \pm vk \qquad (7)$$

and contains massless excitations. This spectrum is radically different from that of the Dirac Hamiltonian appropriate for 2D graphene. Note, in particular, that the linear bands $E_\pm^+$, together with E_+^-, form a triplet (see Fig. 1), following the usual rules for addition of angular momenta with $L = S = 1/2$ and $\vec{J} = \vec{L} + \vec{S}$. This is only natural: assembling pseudospin and spin into a four-component object is equivalent to taking the Kronecker product of two $j = 1/2$ irreducible representations of the SO(3) rotation group, and this product decomposes according the rules of angular momentum composition.[26]

Thus, unlike in 2D where strong spin-orbit interactions simply destroy the orbital Weyl points and turn massless fermions into massive excitations, here we also get Dirac
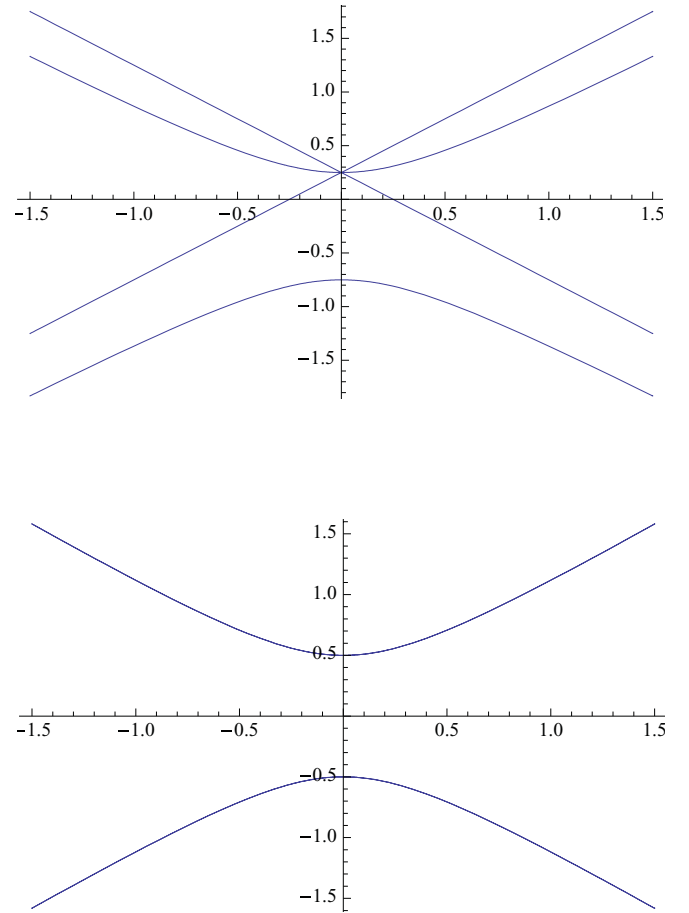

FIG. 1. (Color online) Effects of spin-orbit coupling on the orbital Weyl point of a cubic crystal (top) and graphene (bottom) in arbitrary units.

points with $J = 1$. In the next section we will present a model that in the absence of spin-orbit coupling has, besides orbital Weyl points, Dirac points with pseudospin 1. The points with pseudospin 1 would be split by strong spin-orbit interactions into Weyl points with $J = 1/2$ and novel Dirac points with $J = 3/2$. Subduction of IRs (Refs. 25 and 26) can be used in principle to extend the analysis to noncubic groups.

Henceforth we will assume that spin-orbit interactions are weak and can be ignored. In this limit the dynamics is well described by the 3D Weyl Hamiltonian—albeit with an additional twofold degeneracy due to spin—and, as a consequence, the systems considered in this paper may share some of the properties of Weyl semimetals.

IV. A TIGHT-BINDING EXAMPLE

As a practical application, we present a tight-binding model with space group **214** $I4_132(O^8)$, the first entry in Table I. According to our previous analysis, *any* lattice with this space group must have orbital Weyl points at P. Here we consider a lattice with four atoms per primitive unit cell, with Cartesian coordinates $\vec{r}_1 = (a/8)(1,1,1)$, $\vec{r}_2 = (a/8)(1,\bar{1},3)$, $\vec{r}_3 = (a/8)(3,\bar{1},5)$, and $\vec{r}_4 = (a/8)(3,1,7)$.[29]

With each atom we associate a Bloch function

$$\Phi_i(\vec{k}) = \sum_{\vec{t} \in \mathcal{T}} e^{i\vec{k} \cdot (\vec{r}_i + \vec{t})} \varphi(\vec{r} - \vec{r}_i - \vec{t}), \qquad (8)$$

where the sum runs over all the points in the Bravais lattice and $\varphi(\vec{r})$ is an s-wave atomic orbital. Each atom has three nearest neighbors (NNs), with bonds parallel to the three Cartesian

planes. In terms of the reduced Cartesian components of the wave vector $\vec{k} = (2\pi/a)(k_x, k_y, k_z)$ the NN tight-binding Hamiltonian is given by

$$
H(\vec{k}) = t \begin{pmatrix} 0 & e^{(i\pi/2)(k_z-k_y)} & e^{(i\pi/2)(k_y-k_x)} & e^{(i\pi/2)(k_x-k_z)} \\ e^{-(i\pi/2)(k_z-k_y)} & 0 & e^{(i\pi/2)(k_x+k_z)} & e^{-(i\pi/2)(k_x+k_y)} \\ e^{-(i\pi/2)(k_y-k_x)} & e^{-(i\pi/2)(k_x+k_z)} & 0 & e^{(i\pi/2)(k_y+k_z)} \\ e^{-(i\pi/2)(k_x-k_z)} & e^{(i\pi/2)(k_x+k_y)} & e^{-(i\pi/2)(k_y+k_z)} & 0 \end{pmatrix},
\tag{9}
$$

where $t < 0$ is the hopping parameter and the diagonal on-site energy has been set to zero. The Hamiltonian can be diagonalized numerically and the resulting bands are shown in Fig. 2.

The existence of linear bands at point P is obvious in Fig. 2. We can use standard group theory techniques to confirm that they actually are Weyl points, as predicted. The four Bloch functions Φ_i form the basis of a reducible representation $\mathcal{H}$ that can be decomposed into small IRs as $\mathcal{H}(\Phi_1, \ldots, \Phi_4) = P_2(e_1, e_2) + P_3(u_1, u_2)$. Up to normalizations, the symmetry-adapted vectors are given by $e_1 \sim (1, \beta_2, -1, i\beta_2)$, $e_2 \sim (-\beta_2, -1, -\beta_2, i)$, with $\beta_2 = (1 + \sqrt{3})(1 - i)/2$, and identical expressions for u_1, u_2 with β_2 replaced by $\beta_3 = (1 - \sqrt{3})(1 - i)/2$. Using a unitary transformation U_P to change to the symmetry-adapted basis and expanding around the point P yields

$$
U_P^\dagger H(\vec{k}) U_P = \frac{\pi t}{\sqrt{3}} \begin{pmatrix} \frac{3}{\pi} + \vec{\sigma} \cdot \vec{k} & H_{23}(\vec{k}) \\ H_{23}^\dagger(\vec{k}) & -\frac{3}{\pi} - \vec{\sigma} \cdot \vec{k} \end{pmatrix} + O(k^2),
\tag{10}
$$

where $H_{23}(\vec{k})$ is given by

$$
H_{23}(\vec{k}) = \frac{1}{\sqrt{2}} \begin{pmatrix} k_z & \omega^* k_x - i\omega k_y \\ \omega^* k_x + i\omega k_y & -k_z \end{pmatrix}
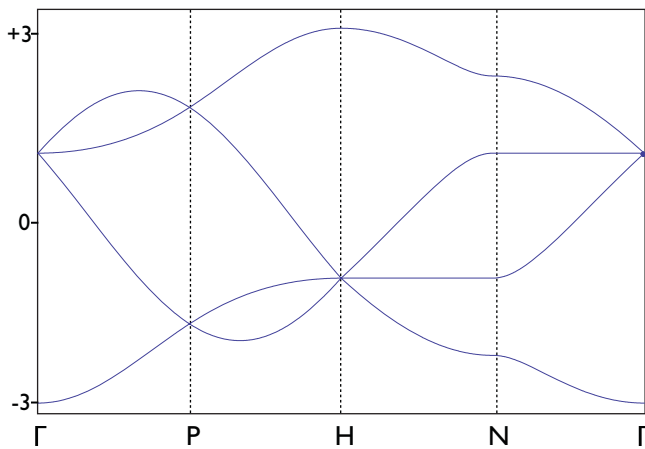\tag{11}
$$

FIG. 2. (Color online) Bands for the cubic lattice in the NN approximation for $t = -1$. The bcc Brillouin zone with its points and lines of symmetry can be seen in Fig. 3.

with $\omega = e^{2\pi i/3}$. There are thus two orbital Weyl points at P with different energies $\pm t\sqrt{3}$ and opposite chiralities. The existence of orbital Weyl points of opposite chirality is of course to be expected from fermion doubling,[30] which requires the net chirality of the BZ to vanish, although the fact that they appear at coincident points is peculiar to this model. Note also the linear couplings between the two points. Due to the split in energies, these couplings contribute corrections $O(k^2)$ to the 2×2 effective Hamiltonians around the orbital Weyl points and do not spoil their structure. A similar expansion around $-\vec{K}_1$ confirms that, due to TRS, each orbital Weyl point is degenerate in energy with another point of the same chirality. Restoration of the lattice constant yields a Fermi velocity $v_F = \frac{a|t|}{2\sqrt{3}}$. Note, however, that, as no symmetry connects the orbital Weyl points with different chiralities and energies, going beyond the NN approximation is expected to give different Fermi velocities for them.

Figure 2 exhibits linear bands around the Γ and H points as well. Their nature is, however, very different from that of the orbital Weyl points at P. Let us consider, for the sake of concreteness, the Γ point. In this case, the representations associated with the Bloch functions decompose into IRs of dimensions 1 and 3, $\mathcal{H} = A_1 + T_2$. Transforming to the appropriate symmetry-adapted basis and linearizing yields

$$
U_\Gamma^\dagger H(\vec{k}) U_\Gamma = t \begin{pmatrix} 3 & 0 & 0 & 0 \\ 0 & -1 & -i\pi k_z & i\pi k_y \\ 0 & i\pi k_z & -1 & -i\pi k_x \\ 0 & -i\pi k_y & i\pi k_x & -1 \end{pmatrix} + O(k^2).
\tag{12}
$$

Up to a constant energy, the 3×3 block can be written

$$
H_{T_2}(\vec{k}) = \pi t \vec{J} \cdot \vec{k},
\tag{13}
$$

where $(J_i)_{jk} = -i\varepsilon_{ijk}$ are spin-1 matrices. Thus, around this Dirac point, electrons behave more like massless spin-1 particles, with spectrum $E(\vec{k}) = 0, \pm v_F|\vec{k}|$ and $v_F = \frac{1}{2}a|t|$. Indeed, one can check that, while the $E = 0$ component is longitudinally polarized, the other two are transverse, just like the propagating components of a photon. Pseudospin-1 Dirac points have been reported in some two-[31–33] and three-dimensional[34] systems.

A look at Fig. 2 shows that, even if the Fermi level coincides with one of the orbital Weyl points at P, band overlap will cause the dynamics to be dominated by large electron (or hole) pockets. The existence of band overlap can be traced in
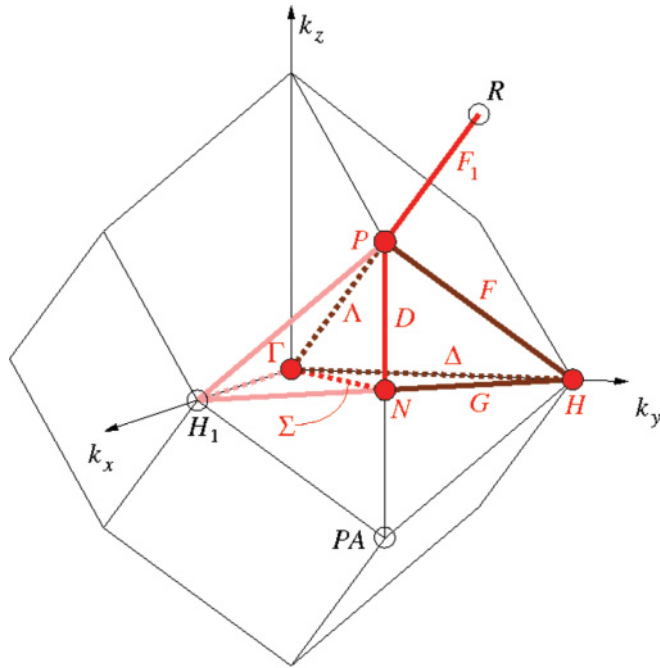
FIG. 3. (Color online) Brillouin zone for bcc crystals (Refs. 27 and 28).

this case to the threefold degeneracies in Fig. 2, which force one of the bands arising from the orbital Weyl points to bend over. As 3d IRs exist only for cubic groups, we may modify the model by making the hopping parameters $t_\perp$ associated with bonds parallel to the OXY plane different from the rest, $t_\perp = \epsilon\, t$. This reduces the symmetry to the tetragonal subgroup **98** $I4_122$ and eliminates the threefold degeneracies at Γ and H. Figure 4 shows the bands for $\epsilon = 0.4$. In the absence of spin-orbit interactions the system would behave like a gapless semiconductor with massless carriers for 1/4 and 3/4 fillings, with positive or negative chirality depending on the filling.

V. DISCUSSION

In this paper we have studied the interplay between crystal symmetry and the existence of bulk chiral fermions in nonmagnetic 3D crystals with weak spin-orbit coupling.
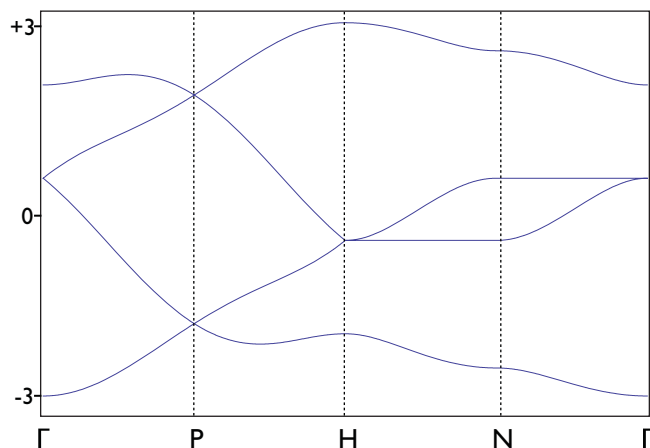

FIG. 4. (Color online) Bands for the cubic lattice with a tetragonal distortion ($\epsilon = 0.4$) for $t = -1.25$. See the main text for details.

We have shown that the space group plays a determinant role, as summarized in Tables I and II. As Weyl semimetals depend on the existence of magnetic order or strong spin-orbit interactions,[15] we have explored an entirely different corner in the space of candidate 3D crystals with bulk chiral fermions. We have also considered the effects of spin-orbit interactions and shown that, unlike in 2D, these may give rise to new critical points supporting massless fermions for different values of the pseudospin. For sufficiently weak spin-orbit interactions the dynamics is well described by the 3D Weyl Hamiltonian and the systems considered in this paper may share some of the properties of Weyl semimetals.

There are two obvious uses for the information in Tables I and II. First, one can look for orbital Weyl points in nonmagnetic crystals with weak spin-orbit interactions and space groups in the tables, either in theoretically computed electronic bands or experimentally. The other use is the design of 3D lattices with Weyl points. This may allow for a physical realization of massless chiral fermions with cold atoms in optical lattices. Note that the physical relevance as well as the feasibility of detecting chiral fermions in actual crystals will be affected by structure-dependent features such as the position of the Fermi level and the amount of band overlap. But knowing that the bulk chiral fermions *have* to be there is obviously a good starting point. As shown in the example of Sec. IV, we can then try to engineer the required properties by modifying the initial system.

There are several possible extensions to this work. One is to consider the existence of orbital Weyl points away from points of symmetry. All the points in a *line* of symmetry, except for the end points, have the same group $\mathcal{G}_{K_1}$. Therefore, symmetry alone cannot imply the existence of bulk chiral fermions at a particular point in the line, although it will indicate whether this is possible at all. But it can, in some cases, imply the existence along the line of "semi-Dirac" points, where the dispersion relations are linear only for some directions. For generic points in the BZ, symmetry alone has little to say and a different kind of analysis may be useful.[35,36]

Sometimes, not two, but three bands become degenerate at a Dirac point.[34] This is the case with the Γ and H points in the example of Sec. IV. This is possible for some cubic space groups, and group theory can be used to determine the IRs and points of symmetry where this may happen. As shown in Sec. III, turning on spin-orbit interactions will give rise to unusual Dirac points with pseudospin 3/2. Other, more complicated, linear Hamiltonians[37–39] are also possible and may be physically relevant. Group theory can be used to classify or even predict the existence of the different types of Dirac point.

In this paper we have analyzed all the single-valued irreducible representations at points of symmetry in the BZ. These are appropriate for orbital degrees of freedom. By considering instead double-valued[26] IRs we could study the existence of Weyl points where the total Hamiltonian, including electron spin and spin-orbit interactions, takes the form of the 3D Weyl Hamiltonian. Thus, we could extend our analysis to TRS-invariant Weyl semimetals. Double-valued IRs have been recently applied to the study of Dirac semimetals.[40]

So far we have restricted ourselves to TRS-invariant crystals. The reasons are mostly practical. The symmetries

of crystals with magnetic order are classified by the 1651 magnetic space groups,[26] instead of the 230 ordinary (Fedorov) space groups that classify crystals with TRS. The amount of work required to examine the points of symmetry and irreducible corepresentations[26] for all the magnetic groups is, obviously, much greater. Moreover, unlike ordinary space groups, there are few databases with the magnetic space groups of crystals with magnetic order.

Nevertheless, some of the results in this paper can also be applied to spinless electrons in crystals with magnetic order. The reason is that, by construction, the 19 entries in Tables I and II describe situations where the 3D Weyl Hamiltonian is invariant under the "gray" or "type II" Shubnikov space group[26] associated with an ordinary (Fedorov) space group by the addition of the TRS operation. Now, all the magnetic space groups derived from the Fedorov space group with the Belov-Neronova-Smirnova (BNS) settings[27,28] are subgroups of the gray group. As a consequence, the corresponding Weyl Hamiltonian is automatically invariant under *all* the magnetic groups derived from the ordinary space groups listed in our tables. For instance, the Weyl Hamiltonians at the P point of group **214** are automatically invariant under the derived magnetic groups **214.68** and **214.69** (in the BNS settings).

One still has to check that the degeneracy of the two bands at the point of symmetry, necessary for the existence of the Weyl point, is maintained under the lower symmetry of the magnetic space group. If this is not the case but the effects of the magnetic order are small, the Weyl point will survive but move away from the point of symmetry. The main difference when dealing with crystals with magnetic order is that we cannot exclude the possibility of finding bulk chiral fermions around points of symmetry for space groups not listed in Tables I and II. That happens whenever the Weyl Hamiltonian is invariant under the magnetic subgroup of the gray space group, but not under the gray space group itself.

APPENDIX

In this Appendix we outline the methods used to obtain Tables I and II and Eq. (2). Symmetry operations belonging to the space group $\mathcal{G}$ will be written $g = \{\alpha|\vec{v}\}$, where α and $\vec{v}$ denote the rotational and translational parts respectively.[26] Let $\{e_i(\vec{K})\}$ be a basis of orbital wave functions that transform linearly under the action of $\mathcal{G}$, $e_i(\vec{K}) \to e_j(\alpha\vec{K})R_{ji}(g)$, where we sum over repeated indices. Invariance of the Hamiltonian under $\mathcal{G}$ means that, for any wave function ψ, $\langle H \rangle_\psi = \langle H \rangle_{\psi_g}$, where ψ_g is the transform of ψ by the group element g. Expanding this condition on the basis $\{e_i(\vec{K})\}$ yields, in matrix

notation,

$$R^\dagger(g)H(\alpha\vec{K})R(g) = H(\vec{K}), \qquad (A1)$$

where $H_{ij}(\vec{K}) = \langle e_i(\vec{K})|H|e_j(\vec{K})\rangle$. Time reversal θ is an antiunitary operation that acts on orbital wave functions by complex conjugation, $e_i(\vec{K}) \to e_i(\vec{K})^* = e_j(-\vec{K})\Theta_{ji}$, where Θ_{ij} is a *unitary* matrix,[24,26] and reverses the momentum $\vec{K}$. Invariance under θ implies

$$\Theta^\dagger H(-\vec{K})\Theta = H^*(\vec{K}). \qquad (A2)$$

We will also have to consider combined antiunitary operations of the form θg. In this case invariance of the Hamiltonian implies

$$T^\dagger(g)H(-\alpha\vec{K})T(g) = H^*(\vec{K}), \qquad (A3)$$

where $T(g) = \Theta R^*(g)$. Equations (A1)–(A3) become powerful constraints on the form of the Hamiltonian when we take $\vec{K} = \vec{K}_1 + \vec{k}$ in the neighborhood of a point of symmetry $\vec{K}_1$ and consider a power expansion in $\vec{k}$.

Consider, for instance, Eq. (A1) with g restricted to the little group of $\vec{K}_1$, $\mathcal{G}_{K_1}$, i.e., $\alpha\vec{K}_1 \equiv \vec{K}_1$

$$R^\dagger(g)H(\vec{K}_1 + \alpha\vec{k})R(g) = H(\vec{K}_1 + \vec{k}). \qquad (A4)$$

By definition, the matrix α belongs to the vector representation V.[24,25] If the basis functions $\{e_i(\vec{K})\}$ belong to the small IR R of $\mathcal{G}_{K_1}$, terms of order n in $\vec{k}$ in an expansion of the left-hand side of Eq. (A4) will transform according to the product $R^* \times R \times [V]^n$, where R^* is the complex conjugate of R and $[V]^n$ denotes the nth symmetric power of the representation V.[24,25] Then one can use standard group theory techniques to determine, order by order in $\vec{k}$, the most general form of the Hamiltonian compatible with the symmetries of the vector $\vec{K}_1$.

In particular, a necessary condition for the existence of the Weyl Hamiltonian, which is linear in $\vec{k}$, is that the vector representation V is contained in the product $R^* \times R$ for some 2d IR (Ref. 42) R of $\mathcal{G}_{K_1}$. We have checked this condition on all the single-valued 2d and 4d IRs at the points of symmetry of the 230 space groups to obtain a first list of candidates.[43] Polar groups have been discarded from the outset, as they couple one component of the momentum to the unit matrix and the result is incompatible with the structure of the Weyl Hamiltonian. The amount of work involved at this stage has been substantially reduced thanks to the use of "abstract groups" in Ref. 26. In essence, the abstract groups represent classes of isomorphic little groups $\mathcal{G}_{K_1}$, and their number is much smaller than the number of little groups.

In the next step each candidate IR has been checked for invariance of the corresponding Hamiltonian under TRS. This involves using Eq. (A2) whenever $-\vec{K}_1 \equiv \vec{K}_1$ and Eq. (A3) if $\vec{K}_1$ is not equivalent to $-\vec{K}_1$ but there exists a space group element $g = \{\alpha|\vec{v}\} \in \mathcal{G}$ such that $-\alpha\vec{K}_1 \equiv \vec{K}_1$. The IRs that pass this last test are listed in the last column of Tables I and II. These IRs have an important property: There is always a basis where the matrices $R(g)$ coincide, up to g-dependent phases, with the $j = 1/2$ rotation matrices

$$R_{1/2}(\hat{n}\phi) = \exp\left(-\frac{i\vec{\sigma}\cdot\hat{n}\,\phi}{2}\right), \qquad (A5)$$

where ϕ is the angle around the unit vector $\hat{n}$. As a consequence, we can always transform to a basis where, up to appropriate rescalings of the components of $\vec{k}$ for nonisotropic crystals [see Eq. (1)], the linear Hamiltonian takes the standard Weyl form $H(\vec{K}_1 + \vec{k}) \simeq v\vec{\sigma} \cdot \vec{k}$.

When $-\vec{K}_1$ is not equivalent to $\vec{K}_1$, the basis at these two points can be related by TRS. Choosing as basis at $-\vec{K}_1$ the complex conjugate of the one at $\vec{K}_1$, i.e., taking as 4d basis (e_1, e_2, e_1^*, e_2^*), and using Eq. (A2), gives $H(-\vec{K}_1 + \vec{k}) \simeq -v\vec{\sigma}^* \cdot \vec{k}$. The off-diagonal blocks between $\vec{K}_1$ and $-\vec{K}_1$ vanish by translation invariance, and we have

$$H(\vec{k}) = v \begin{pmatrix} \vec{\sigma} \cdot \vec{k} & 0 \\ 0 & -\vec{\sigma}^* \cdot \vec{k} \end{pmatrix} + O(k^2). \qquad \text{(A6)}$$

We can make the symmetry between $\vec{K}_1$ and $-\vec{K}_1$ obvious by using the SU(2) transformation $\sigma_y \vec{\sigma}^* \sigma_y = -\vec{\sigma}$ to change

the basis at $-\vec{K}_1$ so that the 4d basis is $(e_1, e_2, ie_2^*, -ie_1^*)$. On this basis the Hamiltonian takes the form given in Eq. (2).

The case $-\vec{K}_1 \equiv \vec{K}_1$ is more subtle, and we have two possibilities. If R is a real 2d IR, then TRS applies (e_1, e_2) onto itself, with $e_i^* = e_i$. In this case, $\Theta = \mathbf{1}$ and Eq. (A2) requires $H(-\vec{k}) = H(\vec{k})^*$, which is not satisfied by the Weyl Hamiltonian. Thus 2d real IRs are excluded from Table I. For complex and pseudoreal 2d IRs and for the real 4d R_3 of **212** and **213**, (e_1^*, e_2^*) are linearly independent of (e_1, e_2). We can take as 4d basis either (e_1, e_2, e_1^*, e_2^*) or $(e_1, e_2, ie_2^*, -ie_1^*)$, and everything proceeds as in the previous case. The main difference is that now the off-diagonal blocks need not vanish by translation symmetry. However, a detailed case by case analysis using space group and TRS invariance shows that the off-diagonal terms are at least of $O(k^2)$. This completes the proof of Eq. (2).

[1] K. S. Novoselov, A. K. Geim, S. V. Morozov, D. Jiang, Y. Zhang, S. V. Dubonos, I. V. Gregorievna, and A. A. Firsov, Science **306**, 666 (2004).

[2] K. S. Novoselov, D. Jiang, T. Booth, V. Khotkevich, S. M. Morozov, and A. K. Geim, Proc. Natl. Acad. Sci. USA **102**, 10451 (2005).

[3] A. H. Castro Neto, F. Guinea, N. M. R. Peres, K. S. Novoselov, and A. K. Geim, Rev. Mod. Phys. **81**, 109 (2009).

[4] M. A. H. Vozmediano, M. I. Katsnelson, and F. Guinea, Phys. Rep. **496**, 109 (2010).

[5] K. L. Lee, B. Grémaud, R. Han, B.-G. Englert, and C. Miniatura, Phys. Rev. A **80**, 043411 (2009).

[6] B. Wunsch, F. Guinea, and F. Sols, New J. Phys. **10**, 103027 (2008).

[7] T. D. Stanescu, V. Galitski, J. Y. Vaishnav, C. W. Clark, and S. DasSarma, Phys. Rev. A **79**, 053639 (2009).

[8] C. L. Kane and E. J. Mele, Phys. Rev. Lett. **95**, 226801 (2005).

[9] M. Z. Hasan and C. L. Kane, Rev. Mod. Phys. **82**, 3045 (2010).

[10] J. L. Alonso, J. A. Capitán, L. A. Fernández, F. Guinea, and V. Martin-Mayor, Phys. Rev. B **64**, 054408 (2001).

[11] P. Hosur, S. Ryu, and A. Vishwanath, Phys. Rev. B **81**, 045120 (2010).

[12] X. Wan, A. M. Turner, A. Vishwanath, and S. Y. Savrasov, Phys. Rev. B **83**, 205101 (2011).

[13] Kai-Yu Yang, Yuan-Ming Lu, and Y. Ran, Phys. Rev. B **84**, 075129 (2011).

[14] Jian-Hua Jiang, Phys. Rev. A **85**, 033640 (2012).

[15] P. Hosur, S. A. Parameswaran, and A. Vishwanath, Phys. Rev. Lett. **108**, 046602 (2012).

[16] G. E. Volovik, *The Universe in a Helium Droplet* (Oxford University Press, Oxford, 2003).

[17] J. L. Mañes, F. Guinea, and M. A. H. Vozmediano, Phys. Rev. B **75**, 155424 (2007).

[18] A. Cortijo, F. Guinea and M. A. H. Vozmediano, eprint arXiv:1112.2054 [J. Phys. A (to be published)].

[19] In some cases translation and other discrete symmetries may be necessary for the existence and stability of the points. See, for instance, Refs. 12 and 17.

[20] J. C. Slonczewski and P. R. Weiss, Phys. Rev. **109**, 272 (1948).

[21] J. L. Mañes, Phys. Rev. B **76**, 045430 (2007).

[22] R. Winkler and U. Zulicke, Phys. Rev. B **82**, 245313 (2010).

[23] E. Kogan and V. U. Nazarov, Phys. Rev. B **85**, 115418 (2012).

[24] G. Y. Lyubarskii, *The Aplication of Group Theory in Physics* (Pergamon, Oxford, 1960).

[25] M. El-Batanouny and F. Wooten, *Symmetry and Condensed Matter Physics: A Computational Approach* (Cambridge University Press, Cambridge, 2008).

[26] C. J. Bradley and A. P. Cracknell, *The Mathematical Theory of Symmetry in Solids* (Clarendon, Oxford, 2010).

[27] M. I. Aroyo, J. M. Perez-Mato, C. Capillas, E. Kroumova, S. Ivantchev, G. Madariaga, A. Kirov, and H. Wondratschek, Z. Kristallogr. **221**, 15 (2006).

[28] M. I. Aroyo, A. Kirov, C. Capillas, J. M. Perez-Mato, and H. Wondratschek, Acta Crystallogr., Sect. A: Found. Crystallogr. **62**, 115 (2006).

[29] We are using Wyckoff position (Refs. 27 and 28) 8*a* because of its relatively low multiplicity.

[30] H. B. Nielsen and M. Nimomiya, Nucl. Phys. **193**, 173 (1981).

[31] D. F. Urban, D. Bercioux, M. Wimmer, and W. Hausler, Phys. Rev. B **84**, 115136 (2011).

[32] N. Goldman, D. F. Urban, and D. Bercioux, Phys. Rev. A **83**, 063601 (2011).

[33] B. Dóra, J. Kailasvuori and R. Moessner, Phys. Rev. B **84**, 195422 (2011).

[34] C. Weeks and M. Franz, Phys. Rev. B **82**, 085310 (2010).

[35] K. Asano and C. Hotta, Phys. Rev. B **83**, 245125 (2011).

[36] C. Sochichiu, e-print arXiv:1112.5937.

[37] S. Y. Zhou, G. H. Gweon, J. Graf, A. V. Fedorov, C. D. Spataru, R. D. Diehl, Y. Kopelevich, D. H. Lee, S. Louie, and A. Lanzara, Nat. Phys. **2**, 595 (2006).

[38] F. Szmulowicz, Solid State Commun. **148**, 410 (2008).

[39] J. C. Smith, S. Banerjee, V. Pardo, and W. E. Pickett, Phys. Rev. Lett. **106**, 056401 (2011).

[40] S. M. Young, S. Zaheer, J. C. Y. Teo, C. L. Kane, E. J. Mele, A. M. Rappe, eprint arXiv:1111.6483 [Phys. Rev. Lett. (to be published)].

[41] http://www.cryst.ehu.es.

[42] The 4d IR R_3 of **212** and **213** is the exception. In this case, the two degenerate chiral fermions belong to a single 4d IR.

[43] We have also examined the "physically irreducible" 2d representations, i.e., pairs of conjugate 1d representations degenerate by TRS. These are never compatible with the Weyl Hamiltonian.